Fig. 7, eine grundsätzlich andere räumliche Anordnung der Chelatringe.

Literatur

Bode, H. & Teufer, G. (1956*a*). *Z. Anorg. Chem.* **283**, 18.

Bode, H. & Teufer, G. (1956*b*). *Acta Cryst.* **9**, 929.

Bond, W. L. (1951). *Rev. Sci. Instrum.* **22**, 344.

Bullen, G. J. (1957). *Acta Cryst.* **10**, 143.

Evans, H. T. & Ekstein, M. G. (1952). *Acta Cryst.* **5**, 540.

Grdenić, D. & Matković, B. (1958). *Nature, Lond.* **182**, 465.

Hargreaves, A. (1957). *Acta Cryst.* **10**, 196.

Hoard, J. L. & Nordsieck, H. H. (1939). *J. Amer. Chem. Soc.* **61**, 2853.

Ibers, J. A. (1956). *Acta Cryst.* **9**, 225.

Ibers, J. A. & Cromer, Don T. (1958). *Acta Cryst.* **11**, 794.

Kiergegaard, P. (1956). *Acta Chem. Scand.* **10**, 599.

Koyama, H., Saito, Y. & Kuroya, H. (1953). *J. Inst. Polytech. Osaka City Univ.* Ser. C, **4**, 43.

Kratky, O. & Krebs, B. (1936). *Z. Kristallogr.* **95**, 253.

Marchi, L. E., Fernelius, W. C. & McReynolds, J. P. (1943). *J. Amer. Chem. Soc.* **65**, 329.

Roof, Raymond B. (1956). *Acta Cryst.* **9**, 781.

Sándor, E. & Gado, P. (1956). *Kristallografiya*, **1**, 729.

Schugam, E. A. (1951). *Doklady Akad. Nauk SSSR*, **81**, 853.

Schugam, E. A. & Schkolnikowa, L. M. (1956). *Kristallografiya*, **1**, Tl. 4, 23.

Shibata, Sh. & Sone, K. (1956). *Bull. Chem. Soc., Japan*, **29**, 852.

Wait, E. & Comyns, A. E. (1958). *Acta Cryst.* **11**, 301.

Wolf, Leopold, & Bärnighausen, H. (1957). *Acta Cryst.* **10**, 605.

Zachariasen, W. H. (1948). *Acta Cryst.* **1**, 265.

Acta Cryst. (1960). **13**, 785

The Crystal Structure of Foshagite

By J. A. Gard and H. F. W. Taylor

Department of Chemistry, University of Aberdeen, Old Aberdeen, Scotland

(*Received* 13 *January* 1960)

The crystal structure of foshagite ($Ca_4(Si_3O_9)(OH)_2$) has been determined from X-ray fibre rotation photographs. It is built from Ca^{+2} and OH^- ions, together with infinite $(SiO_3^{-2})_\infty$ chains similar to those in β-$CaSiO_3$, to which mineral foshagite is closely related structurally. The present results do not support the alternative structure for foshagite, suggested by Mamedov & Belov. Foshagite crystals show partial stacking disorder, and the factors governing the relative stabilities of different stacking arrangements are discussed; the related problem in β-$CaSiO_3$ is also considered. The mechanism of the dehydration process at 700 °C. is discussed.

Foshagite is a fibrous calcium silicate mineral discovered at Crestmore, California, by Eakle (1925). In an earlier paper (Gard & Taylor, 1958), we have shown that its composition is $Ca_4Si_3O_9(OH)_2$ and that it has an *A*-centred monoclinic unit cell with parameters

$$a=10{\cdot}32,\ b=7{\cdot}36,\ c=14{\cdot}07\ \text{Å},\ \beta=106{\cdot}4°,\ Z=4\ .$$

Elongation *b*. Principal cleavage (001).

The dehydration process on heating in air at 700 °C. was also studied; oriented transformation occurs giving β-$CaSiO_3$ and β-Ca_2SiO_4. From the relationship of orientations, and other evidence, it was concluded that the calcium positions in foshagite were similar to those in β-$CaSiO_3$ and also that wollastonite-like chains occurred, thus giving the constitutional formula stated above. On this basis a trial structure was proposed (Taylor, 1958; Gard, Taylor & Staples, 1958; Gard & Taylor, 1959), and preliminary calculations suggested that this was essentially correct. The axes previously reported were confirmed, but the structure was shown to be only geometrically monoclinic. It was concluded that the true space group was $P\bar{1}$.

Foshagite shows partial stacking disorder and provides an example of an O–D structure (Dornberger-Schiff, 1956). The unit cell given above relates to a particular stacking modification; subsequent work, described in this paper, shows that at least one other such modification predominates in some synthetic crystals. It will therefore be found convenient in future to refer indices and atomic coordinates to a geometrically monoclinic structural element with

$$a=10{\cdot}32,\ b=7{\cdot}36,\ c=7{\cdot}04\ \text{Å},\ \beta=106{\cdot}4°,\ Z=2\ .$$

Infra-red absorption studies have been made by Tarte (1959). The results confirmed that the water occurred as hydroxyl coordinated to calcium and not to silicon. The spectrum as a whole showed similarities to those of both α- and β-$CaSiO_3$. Material which had been heated at 800 °C. was also studied; a composite pattern of β-$CaSiO_3$ and β-Ca_2SiO_4 was obtained. This confirms the X-ray results.

The trial structure has now been refined in so far as the experimental data permit, and the present paper deals with the results of this work. It includes also discussion of an alternative structure proposed by Mamedov & Belov (1958), and further discussion of the mechanism of the dehydration process.

Material and experimental data

Foshagite has so far been found to occur only at the original locality, as fibrous aggregates with random orientation of the crystallites around *b*. Only fibre rotation photographs have therefore been obtained. Foshagite is easily synthesized, but the very small crystals so obtainable are even less suitable for precise X-ray work.

X-ray fibre rotation photographs were obtained using 6 cm. and 11·46 cm. diameter cameras with filtered copper radiation. Intensities of the *h0l* and *h2l* reflections were estimated visually by comparison with calibrated intensity strips; the *h0l* intensities were also measured using a microdensitometer, which gave closely similar results. Lorentz, polarization, and Cox & Shaw factors were applied in the usual way. In the case of the *h0l* reflections, a correction was also made for the streaking along lines of constant θ caused by lack of parallelism of the crystallites. The layer lines with *k* odd were weak and continuously streaked along the layer lines; no attempt was made to measure intensities of these reflections, but their geometry has been determined using electron diffraction (Gard & Taylor, 1958).

Even when the 11·46 cm. diameter camera was used, a number of reflections were multiple and could not be resolved. In each case, in estimating observed structure amplitudes for use in the Fourier syntheses, the observed intensity (after correction for geometrical factors) was divided up in the ratio of the squares of the calculated structure amplitudes. This ratio was varied as refinement advanced. Because of difficulties arising from this source, coupled with uncertainties in indexing, reflections with ξ-values above 0·9 were of little use in the structure determination.

A preliminary electron-diffraction study has been made of several crystals from a synthetic preparation of foshagite; the results are described later.

Consideration of Mamedov & Belov's structure

Before refinement could be attempted it was necessary to decide whether the provisional structure already proposed by ourselves or that suggested by Mamedov & Belov (1958) was more nearly correct. They suggested that the constitutional formula was $Ca_8(Si_6O_{17})(OH)_6$, implying the presence of double chains similar to those found in xonotlite ($Ca_6(Si_6O_{17})(OH)_2$; Mamedov & Belov, 1955, 1956*a*). This structure corresponds to the composition $4\,CaO.3\,SiO_2.1\frac{1}{2}\,H_2O$, but no evidence in support of the higher water content was given. It was proposed on general crystal-chemical grounds together with a reinterpretation of the dehydration results of Gard & Taylor (1958). No evidence from X-ray intensities was cited.

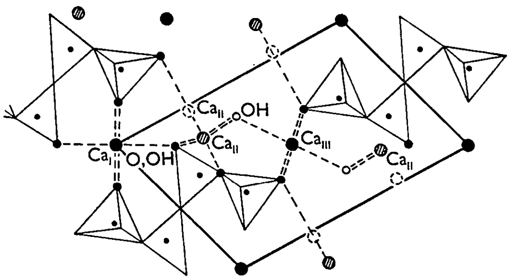

Fig. 1. (010) projection of a structure for foshagite proposed by Mamedov & Belov (1958). The coordination of the calcium ions is as stated in their paper. Broken circles show revised positions for the Ca$_{II}$ ions to give more plausible Ca–O distances. *R* for the first 36 *h0l* reflections was 0·49 before revision and 0·62 after. ⬤ calcium ions at $y = \frac{3}{8}, \frac{7}{8}$. ▨ calcium ions at $y = \frac{1}{8}, \frac{5}{8}$. ● oxygen atoms bonded directly to Si. ○ hydroxyl ions. • Si atoms.

Coordinates for Mamedov & Belov's structure were obtained by measurement of Fig. 1 of their paper, which is essentially the same as Fig. 1 of this paper. Structure factors were calculated for the 36 *h0l* reflections of lowest θ values for each of the alternative structures. For Gard & Taylor's trial structure, the reliability factor $R = \Sigma||F_c|-|F_o||/\Sigma|F_o|$ was 0·26, while for Mamedov & Belov's it was 0·49. Comparisons for individual reflections (Fig. 2) also support Gard & Taylor's structure. Fig. 1 represents an admittedly idealized structure, and some of the interatomic distances appeared improbable. To give more normal bond lengths and possibly better agreement, one pair of calcium atoms was moved as shown in Fig. 1 and structure factors again calculated. Agreement with the observed values was, however, even worse than before; *R* rose to 0·62 (Fig. 2(*e*)). The Ca–O bonds shown in Fig. 1 were deduced from the octahedra in Fig. 3 of Mamedov & Belov's paper; the coordinations of individual calcium atoms do not obey Pauling's electrostatic valency rule.

Further criticisms may be made of Mamedov & Belov's structure. It implies a higher water content than does that of Gard & Taylor, and this cannot be reconciled with the observed thermal weight-loss curve (Gard & Taylor, 1958). This curve showed two steps which could be quantitatively explained in terms of thaumasite (known to be present as an impurity) and foshagite, provided that the latter is assumed to have the composition $4\,CaO.3\,SiO_2.H_2O$. The steps cannot possibly be explained quantitatively in terms of a composition $4\,CaO.3\,SiO_2.1\frac{1}{2}\,H_2O$, whatever proportion of thaumasite is assumed to be present.

In principle, it might be possible to distinguish between the two formulae by measurement of the density, but the difference between the values calculated for the two structures is only 0·06. In view of the contamination of the material by thaumasite, which is of very low density (1·88 g.cm.$^{-3}$), this does not seem a reliable method for testing the two hypotheses.

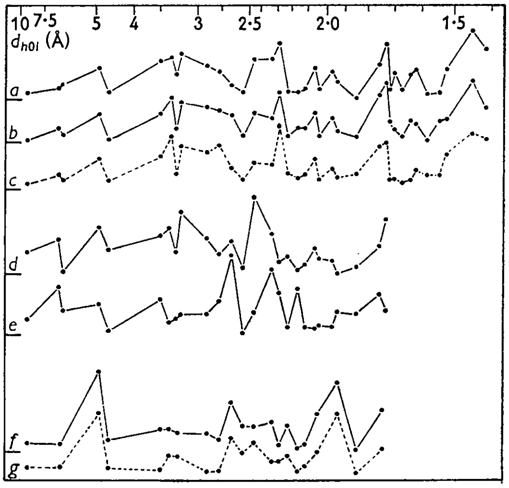

Fig. 2. Comparison of observed structure factors $|F_o|$ with those calculated for the two structures proposed for foshagite. (*a*) $|F_c|$ for *h0l* reflections of the trial structure of Gard & Taylor (1959), and (*b*) the same after refinement. (*c*) (broken lines) $|F_o|$ for the *h0l* reflections. (*d*) and (*e*) $|F_c|$ for *h0l* reflections of the trial structure of Mamedov & Belov (1958), before and after revision of Ca_{II} positions respectively. (*f*) $|F_c|$ for *h2l* reflections of the refined structure of Gard & Taylor. (*g*) (broken lines) $|F_o|$ for the *h2l* reflections. Reflections, some of which are multiple, are in the same order as in Table 2.

Mamedov & Belov considered that their proposed structure explained the observed behaviour on dehydration more simply than did that of Gard & Taylor. This is discussed later. In the meantime, the evidence against their structure appears to be strong, and Gard & Taylor's trial structure was therefore used as a basis for refinement.

Determination of the structure

The trial structure has already been described (Gard & Taylor, 1959) and differs only in detail from the refined structure shown in Figs. 3 and 4(*c*); the most important shift that occurred on refinement was one of Ca_{II} by about 0·2 Å. A high degree of refinement could not be expected, in view of the limited number and precision of the observed structure amplitudes, and the fact that refinement was possible only for the *h0l* projection. As a first approximation it was assumed that a centre of symmetry is present, and that with certain exceptions all atoms occur twice in the height of the projection. The exceptions are Si_I and O_{VI} which only occur once (Figs. 3 and 4(*c*)). The hydroxyl ions coincide in projection with O_I and O_{II}.

There were successively performed an F_o synthesis using 18 selected reflections, an $F_o-(F_{Ca}+F_{Si})_c$ synthesis, and a further F_o synthesis. This third synthesis, results of which are shown in Fig. 3, employed 35 out of the 36 *h0l* reflections whose *d*-spacings exceeded 1·74 Å, as their phases seemed to be adequately established. During the refinement, *R* fell from 0·26 to 0·18 for these 36 reflections, and from

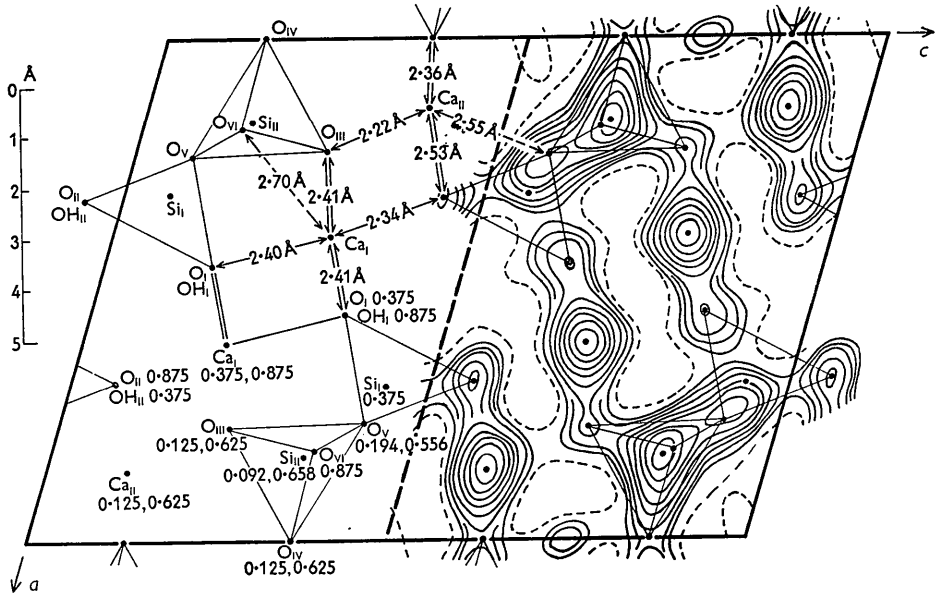

Fig. 3. Electron-density map for (010) projection of foshagite. The broken contour is at 4 e.Å^{-2}; lower contours are omitted. The first solid contour is at 6 e.Å^{-2}; others are at intervals of 2 e.Å^{-2} round the calcium atoms, and 1 e.Å^{-2} elsewhere. Typical *y*-parameters and Ca–O distances are shown on the left. The *A*-centred cell is shown in full lines; the broken line divides it into two structural elements.

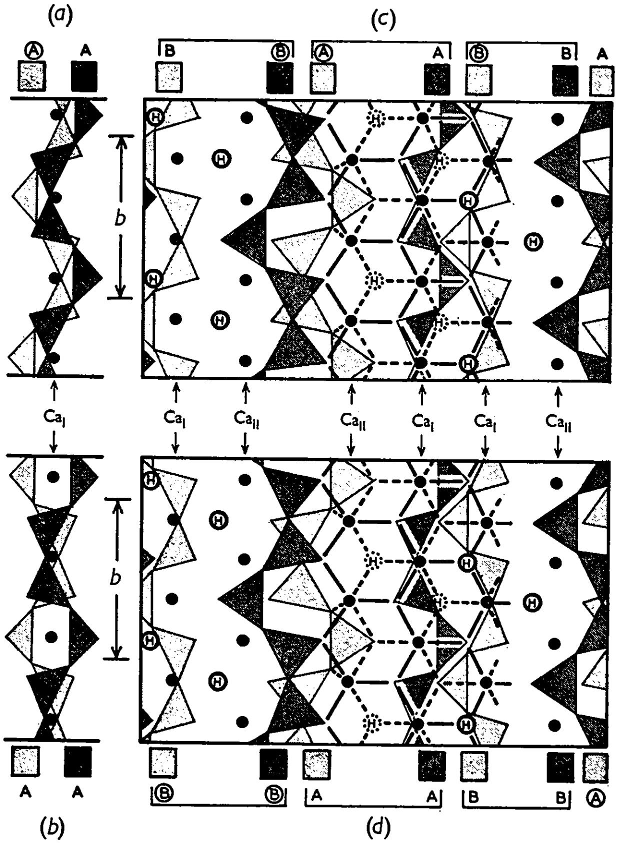

Fig. 4. Projections on the calcium ion planes of parts of the structures of β-CaSiO$_3$ and foshagite. (*a*) Row of Ca$_I$ ions with adjoining Si–O chains in observed modifications of β-CaSiO$_3$. (*b*) The same for non-observed modifications. (*c*) Ca ion sheets with adjoining Si–O chains in observed modifications of foshagite. (*d*) The same for non-observed modifications. In all cases, full circles denote Ca ions, and shaded triangles represent Si–O tetrahedra; only those faces of the tetrahedra which are adjacent to the Ca ions are shown. [*H*] and ⟨*H*⟩ denote hydroxyl ions, and lines, Ca–O bonds; in Fig. 4 [*H*] and ⟨*H*⟩ are indicated as inscribed in circles having full and dotted circumferences respectively. Full circles or lines, and heavy shading, represent parts of the structure in front of the calcium ion planes, while broken circles or lines, and light shading, represent parts behind them. For explanation of symbols *A*, *B*, [*A*], and [*B*], and of the brackets linking them together, see text.

0·29 to 0·23 for the 58 reflections with *d*-spacings above 1·4 Å. The significance of *R* for the extended range of reflections is, however, somewhat doubtful because of some uncertainties in indexing. In an attempt at further refinement an F_o synthesis was performed using all 58 reflections, but the results were unsatisfactory. The main reason for this was undoubtedly the occurrence in the rotation photograph of two strong peaks with *d*-spacings of 1·40 and 1·45 Å, which consisted respectively of five and six unresolved reflections. It was concluded that the results of the previous synthesis, using 35 reflections, represented all the information reliably obtainable from the available data. Most of the atoms are resolved in the final projection (Fig. 3), and the electron density does not drop below $-1{\cdot}5$ e.Å^{-2}. Integrated minimum cross-sections of the most prominent peaks corresponded to atomic numbers of about 34 for each pair of calcium ions, and 29 for the peak containing two Si$_{II}$ and one O$_{VI}$ atoms. The rather low values, compared with the theoretical ones of 36 for each peak, may be explained by the limited number of reflections used in the synthesis. No attempt was made to refine the *y*-parameters; *R* for the first 36 *h*2*l* reflections fell during refinement only from 0·29 to 0·28. The *y* coordinates are therefore probably less precisely determined than are *x* and *z*. In deciding on the final atomic coordinates, the results of the Fourier projection were used as far as possible. This gave values close to 1·60 Å for those Si–O distances which could be directly determined; the Si$_I$, O$_V$ and O$_{VI}$ positions, which were doubtful, were chosen so that the remaining Si–O distances were also close to this value. The final atomic coordinates are listed in Table 1, and structure factors calculated from these coordinates are compared with the observed ones in Table 2.

Table 1. *Atomic coordinates for the structural element with* $a = 10{\cdot}32$, $b = 7{\cdot}36$, $c = 7{\cdot}04$ Å, $\beta = 106{\cdot}4°$

	x	*y*	*z*
Ca$_I$	0·392	0·125, 0·625	0·600
Ca$_{II}$	0·140	0·375, 0·875	0·780
Si$_I$	0·308	0·125	0·117
Si$_{II}$	0·167	0·408, 0·842	0·296
O$_I$	0·450	0·125	0·292
OH$_I$	0·450	0·625	0·292
O$_{II}$	0·317	0·125	−0·116
OH$_{II}$	0·317	0·625	−0·116
O$_{III}$	0·225	0·375, 0·875	0·525
O$_{IV}$	0·010	0·375, 0·875	0·267
O$_V$	0·234	0·306, 0·944	0·150
O$_{VI}$	0·175	0·625	0·267

Description of the structure

The essential features are shown in Figs. 3 and 4(*c*). The results confirm the presence of Ca^{+2} and OH$^-$ ions, together with $(\mathrm{SiO}_3^{-2})_\infty$ chains closely resembling those in wollastonite (Dornberger-Schiff, Liebau & Thilo, 1955; Mamedov & Belov, 1956*b*; Buerger, 1956; Tolliday, 1958). The close relationship between the structures of foshagite and wollastonite, or β-CaSiO$_3$, has already been emphasized (Gard & Taylor, 1959) and will not be further discussed. The Ca ions in foshagite lie almost in sheets parallel to (101) of the structural element, but they are not quite coplanar. Rows of calcium ions parallel to *b* are separated by 2·94 Å for Ca$_I$–Ca$_I$, 3·20 Å for Ca$_I$–Ca$_{II}$, and 4·82 Å for Ca$_{II}$–Ca$_{II}$. Coordination of all the Ca ions is partly by O and partly by OH, and always approximates to octahedral; the structure can thus be alternatively described in terms of distorted octahedral layers of

Table 2. *Comparison of calculated and observed structure factors*

Reflections are listed in order of *d*-spacings, as $|F_o|$ cannot always be given for individual reflections
For multiple reflections, $|F_c| = (\Sigma (F_c)^2)^{\frac{1}{2}}$

	$k=0$			$k=2$		
hkl	F_c	$\|F_c\|$	$\|F_o\|$	F_c	$\|F_c\|$	$\|F_o\|$
$1k0$	+3		8	+11		17
$0k1$	−22		21	+6	9	22
$1k\bar{1}$	+15		13	−6		
$2k0$	−36	39	40	+103	104	89
$1k1$	+15			+10		
$2k\bar{1}$	−5		13	−13		18
$2k1$	−23	38	44	−10	29	14
$1k\bar{2}$	−30			−27		
$3k\bar{1}$	−17	59	68	−4	29	32
$0k2$	−57			−29		
$3k0$	−22		22	−17	25	30
$2k\bar{2}$	−57		57	−18		
$1k\bar{2}$	−49		46	−23		12
$3k\bar{2}$	+45		56	−18		12
$3k1$	+34		28	+64		57
$4k\bar{1}$	−6		12	−33		37
$4k0$	−29	40	36	−4	32	49
$2k2$	+28			−32		
$1k\bar{3}$	−29	33	32	+10	38	23
$4k\bar{2}$	+17			−37		
$2k\bar{3}$	+68		82	−3		23
$0k3$	−6		18	+33		31
$3k\bar{3}$	−18		14	+4		14
$4k1$	+22		18	+9		20
$3k2$	+41		40	−16	48	36
$1k3$	+10	16	12	−32		
$5k\bar{1}$	−13			−33		
$5k0$	+35		27	−38	94	86
$5k\bar{2}$	+13	16	16	+61		
$4k\bar{3}$	+9			+61		
$2k3$	−8		18	+3		< 14
$4k2$	+16	64	56	+40	52	43
$5k1$	−62			+24		
$1k4$	+79	82	58	+4		
$2k\bar{4}$	+23			+7		
$5k\bar{3}$	+7			−20		
$60\bar{1}$	+27		< 12			
$30\bar{4}$	−18		< 12			
004	+2	6	< 12			
$60\bar{2}$	−6					

	$k=0$		
hkl	F_c	$\|F_c\|$	$\|F_o\|$
303	+9	27	< 12
600	+26		
$40\bar{4}$	−25		22
104	−1		16
$60\bar{3}$	−25		16
502	−18	30	46
$50\bar{4}$	−25		
204	−6	86	75
403	−23		
601	+11		
$70\bar{1}$	+42		
$70\bar{2}$	−70		
$10\bar{5}$	−23		
$20\bar{5}$	+1	42	65
$30\bar{5}$	+6		
$60\bar{4}$	+15		
700	+28		
$70\bar{3}$	+12		

composition $Ca(O, OH)_2$ parallel to (101), between which lie the silicon and remaining oxygen atoms.

The following discussion on the coordination of the calcium ions relates to the predominant stacking modification which can be referred to the *A*-centred geometrically monoclinic cell already described; the position for other stacking modifications is discussed later. Ca–O bonds, with distances possibly accurate to 0·05 Å, are shown in Figs. 3 and 4(*c*). The $\mathrm{Ca_{I}}$ ions are coordinated by four oxygen atoms and two hydroxyl ions at 2·34–2·41 Å in a distorted octahedron. Each of the oxygens is linked also to one silicon, and oxygens and hydroxyls alike are linked to two other calciums. Pauling's electrostatic valency rule is thus obeyed. Alternate $\mathrm{Ca_{I}}$ ions in the height of the projection have in addition $\mathrm{O_{VI}}$ 2·70 Å away. This distance might be considered short enough to constitute a bond, but for the fact that $\mathrm{O_{VI}}$ is also linked to two silicons. The $\mathrm{Ca_{II}}$ ions are surrounded by five oxygens and one hydroxyl at 2·22–2·55 Å, which in turn are coordinated as follows. $\mathrm{O_{V}}$ is bound to two silicons. The hydroxyl and the oxygen at $\mathrm{O_{II}}$ are each linked to two more calciums, and in the case of the oxygen to one silicon as well. The oxygen at $\mathrm{O_{III}}$ is also linked to two more calciums and one silicon. The two oxygens at $\mathrm{O_{IV}}$ are each linked to only one more calcium, and one silicon. Pauling's rule is obeyed if the $\mathrm{Ca_{II}}$–$\mathrm{O_{V}}$ bond is assumed to have zero strength, since the two $\mathrm{Ca_{II}}$–$\mathrm{O_{IV}}$ bonds each have strength $\frac{1}{2}$ and the three remaining bonds each have strength $\frac{1}{3}$. This discussion of electrostatic bond strength follows that of Tolliday (1958) for the analogous case of parawollastonite.

The satisfactory course of the structure determination shows that the assumption of a centre of symmetry was justified, at least to the degree of accuracy attainable with the experimental data. It is possible that, as with parawollastonite (Tolliday, 1958), small deviations from an idealized structure cause the structure to be not quite centrosymmetric. More precise experimental data, obtained on better material than is now available, would be needed to detect this.

For convenience, the *A*-centred monoclinic unit cell has been used throughout the above discussion. Inspection of the structure shows, however, that there is no symmetry other than the centre. A triclinic cell can be chosen with contents $2[Ca_4Si_3O_9(OH)_2]$ and

$$a = 10{\cdot}32,\ b = 7{\cdot}36,\ c = 7{\cdot}94\ \text{Å};$$
$$\alpha = 117{\cdot}6^\circ,\ \beta = 104{\cdot}5^\circ,\ \gamma = 90^\circ.$$

This cell is formally correct, but is much less convenient to use than the geometrically monoclinic one.

Stacking modifications in foshagite

Stacking disorder is possible in foshagite because there are two alternative positions, separated by $b/2$, for each metasilicate chain; the situations of the hydroxyl ions are decided by those of the chains (Fig. 4). In principle, an infinite number of modifications is permissible. In fact, the electron-diffraction results show that two predominate in the natural and synthetic crystals so far examined, and that certain possibilities are almost wholly excluded. It will be convenient to refer all modifications to geometrically monoclinic axes parallel to those of the structural element, using multiple values of *a* or *c* or both where necessary. This will entail the use of unconventional concepts such as *F*-centred geometrically monoclinic cells, but avoids the use of triclinic axes which are cumbersome and

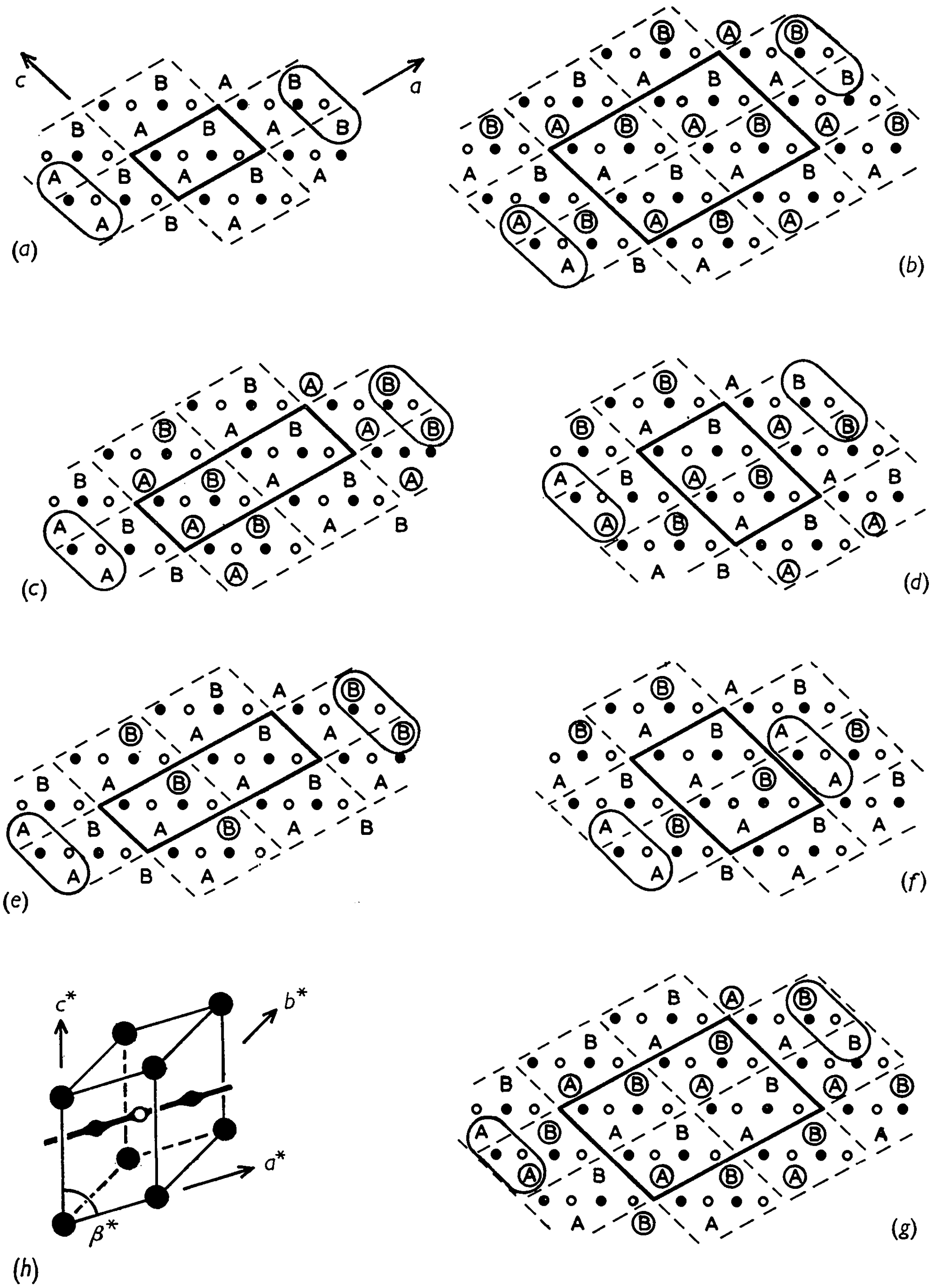

Fig. 5. (010) projections of possible stacking modifications of foshagite. (*a*), (*c*), (*e*), and (*f*) primitive or *C*-centred modifications. (*b*), (*d*), and (*g*) *A*- or *F*-centred modifications. ● Ca at $\frac{3}{8}$ and $\frac{7}{8}$. ○ Ca at $\frac{1}{8}$ and $\frac{5}{8}$. *A*, [*B*], [*A*], *B* represent metasilicate chains with their single Si atoms at $\frac{1}{8}$, $\frac{3}{8}$, $\frac{5}{8}$, $\frac{7}{8}$ respectively. Some pairs of these symbols are ringed together; for significance, see text. Thin, broken lines outline structural elements; thick, full lines outline unit cells. (*h*) Reciprocal cell from electron diffraction. Large, full circles represent pseudo-cell reflections given by all stacking modifications. The streaks, parallel to a^*, were also observed with all crystals. Small full and open circles represent maxima on them corresponding respectively to the *A*- and *F*-centred modifications discussed in the text.

obscure the relationships between the various modifications. Also for convenience, unit-cells will sometimes be used with centres of symmetry not on the origin.

Information about the stacking modifications is provided by the weak reflections with k odd, the positions of which in reciprocal space are shown in

Fig. 5(*h*). In the natural crystals, these reflections have their maxima on the *A*-centres of the reciprocal cell. In the electron-diffraction study of synthetic foshagite already referred to, some of the crystals were also found to have their maxima at the *A*-centres, but others had them at the body centres, and with yet other crystals, maxima occurred at both of these positions.

In the first case, the real cell is geometrically monoclinic, *A*-centred, with doubled *c*; in the second, it is geometrically monoclinic, *F*-centred, with doubled *a* and *c*;† in the third, ordered regions with both of these kinds of stacking occur in the same crystal.

In both natural and synthetic crystals, streaks occur in the reciprocal lattice, principally as shown in Fig. 5(*h*), indicating stacking disorder. The positions of the streaks show that all parts of the crystal are *A*-centred, but that over many small regions stacking modifications occur that have arbitrary multiple values of *a*. Streaks parallel to c^* in the reciprocal lattice of natural crystals (Gard & Taylor, 1958) are so much weaker that modifications which are not *A*-centred make only a very minor contribution to the structure.

For convenience in the ensuing discussion, metasilicate chains with the single silicon atom (Si_I in Fig. 3) at $y=\frac{1}{8}$, $\frac{3}{8}$, $\frac{5}{8}$, and $\frac{7}{8}$ are represented *A*, [*B*], [*A*], and *B* respectively. In the Figs., [*A*] and [*B*] are indicated as *A* and *B* inscribed in circles. Figs. 5(*a*)–(*g*) show some of the simplest real or hypothetical stacking modifications; in the horizontal rows between calcium ions, only the sequences

$$ABAB\ldots,\ AB[A][B]\ldots,\ \text{and}\ ABA[B]\ldots$$

have been considered. For each modification, it was further assumed that all such rows were given by projection of the same sequence in either the *a*- or *c*-direction, but that alternate rows may also be displaced bodily by $b/2$ in the *b*-direction (e.g. Figs. 5(*b*) and (*g*)). The sequence *ABAB*... thus gives the modifications (*a*) and (*b*); sequence *AB*[*A*][*B*]... gives (*c*) and (*d*); sequence *ABA*[*B*]... gives four possible modifications, of which three are shown ((*e*), (*f*), and (*g*)). The *A*-centred modifications are (*b*), (*d*), and (*g*). Of these, (*d*) is the simple *A*-centred one which predominates in the natural mineral and in some synthetic crystals, while (*b*) is the *F*-centred one that predominates in other synthetic crystals. (*g*) is one of the many other modifications that may be supposed to exist in small regions of partly disordered material. The other modifications shown in Fig. 5((*a*), (*c*), (*e*) and (*f*)) are not *A*-centred and may be supposed to contribute to only a very minor extent to the structure.

In Figs. 4(*c*), 4(*d*), and 5, pairs of chains are bracketted or ringed together to show that, in any *A*-centred modification, *A* alternates with [*A*], and *B* with [*B*], in the *c*-direction. In the non *A*-centred modifications, *A* alternates with *A*, or *B* with *B*, in parts or all of the structure. Reference to Fig. 4(*c*) shows that, where *A* alternates with [*A*], and *B* with [*B*], each Ca_I ion is coordinated to four oxygens and two hydroxyls. Where *A* alternates with *A*, and *B* with *B* (Fig. 4(*d*)), some Ca_I ions are coordinated by five oxygens and one hydroxyl, while others are coordinated by three oxygens and three hydroxyls.

The main feature common to all the important stacking modifications thus appears to be equalization of the number of hydroxyls coordinated to each Ca_I ion. No detailed explanation for this is offered, but the relative polarizations of hydroxyl ions and oxygen atoms bonded to the calciums may produce forces that favour this condition.

This theory does not explain why the simple *A*-centred modification predominates in the natural mineral over others centred on the *A*-face, of which the *F*-centred form (Fig. 5(*b*)) is a special case. The predominance of the latter form in some synthetic crystals suggests that the energy differences between these different *A*-centred forms are small. Other modifications within the *A*-centred group may possibly later be found to occur in nature. In this event, we hope that no new mineral names will be proposed. The introduction of such names as parawollastonite to denote stacking modifications is to be deprecated.

Stacking modifications in β-$CaSiO_3$

Earlier workers (Jeffery, 1953; Dornberger-Schiff, Liebau & Thilo, 1955) have accounted for the fact that different stacking modifications of β-$CaSiO_3$ exist, but have not explained why the observed ones predominate. The explanation cannot be the same as for foshagite, as no hydroxyl ions are present. The two cases nevertheless have features in common which make it of interest to discuss that of β-$CaSiO_3$.

The only fully ordered modifications known are wollastonite (Fig. 6(*b*)) and parawollastonite (Figs. 6(*a*) and (*e*)). The unit cell of parawollastonite is primitive monoclinic, with

$$a=15\cdot417,\ b=7\cdot321,\ c=7\cdot066\ \text{Å},\ \beta=95\cdot4^\circ$$

(Tolliday, 1958). By analogy with foshagite, and for similar reasons, all stacking modifications will be referred to geometrically monoclinic axes parallel to those of parawollastonite, using multiple values of *a* or *c* or both where necessary. The unit cells thus defined sometimes differ from the conventional ones; the projection of the conventional, triclinic cell of wollastonite, for instance, is shown in Fig. 6(*b*) in thick, broken lines.

Jeffery (1953) found that, in β-$CaSiO_3$ crystals with partial stacking disorder, all reflections with *k* odd were streaked parallel to a^*. There were maxima on these streaks corresponding to both wollastonite and

---

† The equivalent triclinic cell has space group $P\bar{1}$, and $a=10\cdot96$, $b=7\cdot36$, $c=7\cdot94$ Å; $\alpha=117\cdot6$, $\beta=94\cdot3$, $\gamma=109\cdot6^\circ$.

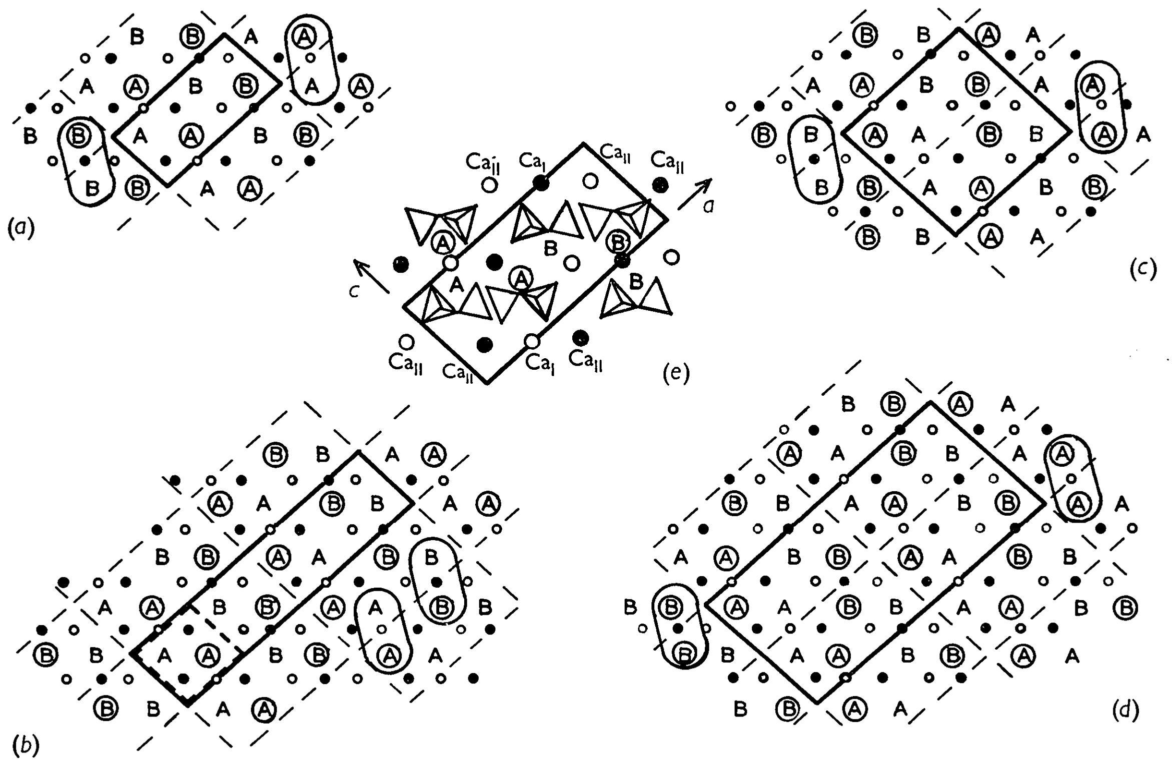

Fig. 6. (010) projections of various stacking modifications of β-$CaSiO_3$. (*a*) Parawollastonite. (*b*) Wollastonite. (*c*), (*d*) Hypothetical forms with doubled *c* (see text). (*e*) Enlarged projection of parawollastonite. Conventions are similar to those in Fig. 5, with the addition of heavy, broken lines in Fig. 6(*b*) to denote the projection of the conventional, triclinic cell.

parawollastonite. This means that the crystals contain ordered regions with both of these structures, and also many small regions where *a* has various multiple values; *c*, however, is never multiple. It therefore appears that the feature common to all the observed modifications is the absence of multiple values of *c*. Figs. 6(*a*)–(*d*) show the four simplest real or hypothetical stacking modifications for β-$CaSiO_3$. The observed ones ((*a*) and (*b*)) have *c* as in parawollastonite; (*c*) and (*d*), which each have doubled *c*, are not observed.

In the observed forms the single Si atoms in metasilicate chains always lie at different heights (*A* and [*A*], or *B* and [*B*]) at opposite sides of a row of Ca_I ions (the atoms are numbered as in Fig. 6(*e*)). In any form with doubled c, at least some of these chains would lie at the same height. Pairs of chains are ringed together in Fig. 6 to clarify this point. When the chains lie at different heights each Ca_I ion in the row has only one near oxygen which is also linked to two silicons (Fig. 4(*a*)). If they were at the same height, half of these Ca_I ions would have two such near oxygens, and the others none (Fig. 4(*b*)). Maximum stability thus appears to be attained when all the Ca_I ions have the same coordination. Repulsive forces may exist between a cation and an oxygen linked to two silicons, and accommodation of these forces may only be possible when not more than one such oxygen is near the cation.

This theory explains why the observed stacking modifications exist, and no others, but it does not predict anything about the relative stabilities of wollastonite and parawollastonite. The effect is not relevant to the case of foshagite, where half the Ca_I ions always have one near oxygen atom linked to two silicons and the others none (Figs. 4(*c*) and (*d*)). In β-$CaSiO_3$, the observed modifications have greater distances between the single Si atoms of neighbouring chains than do those that are not observed, but these distances are in any case so large that this effect seems unlikely to be important.

Dehydration

As has previously been mentioned, dehydration of foshagite causes oriented transformation to β-$CaSiO_3$ and β-Ca_2SiO_4. X-ray patterns of dehydrated fibres always show a strong, oriented pattern of β-$CaSiO_3$, but the relative strength of the β-Ca_2SiO_4 pattern varies from fibre to fibre, and sometimes it is absent. Attempts to detect β-Ca_2SiO_4 by electron diffraction have so far been unsuccessful. Both products when formed show preferred orientation, foshagite *b* becoming both β-$CaSiO_3$ *b* and β-Ca_2SiO_4 *b*. Gard & Taylor

(1958) concluded that preservation of orientation around this axis occurred with the β-$CaSiO_3$, but probably not with the β-Ca_2SiO_4.

We have previously reported that the β-$CaSiO_3$ formed on dehydration of foshagite is a mixture of wollastonite and parawollastonite. Subsequent closer examination of the electron-diffraction patterns showed that these layers consist of quite dense continuous streaks in the a^* direction, sometimes with weak maxima. Where these are sufficiently resolved, they correspond to the twinned triclinic form of wollastonite rather than to parawollastonite.

The formation of completely oriented β-$CaSiO_3$ is simply explained on the hypothesis of silicon migration originally suggested to account for the analogous transformation of xonotlite into β-$CaSiO_3$ (Dent & Taylor, 1956). As has already been explained (Gard & Taylor, 1959), the structures of both foshagite and β-$CaSiO_3$ can be described in terms of distorted octahedral layers of composition $Ca(O, OH)_2$, between which occur the silicon and remaining oxygen atoms. This is also true of xonotlite. Both of the transformations under consideration can be explained if the element of the structure that persists is the distorted $Ca(O, OH)_2$ layer. In order to convert foshagite into β-$CaSiO_3$, the only reconstructive changes necessary (excepting expulsion of protons) are ones that involve only the silicon and oxygen between the octahedral layers; more silicon and oxygen must be introduced into these lamellar spaces, and the hydrogen must move out. It may be supposed that some parts of the structure, previously described as donor regions (Gard & Taylor, 1958) supply these silicon and oxygen atoms, and also more oxygen to combine with the hydrogen, forming water.

The weakness of the β-Ca_2SiO_4 pattern, and its probably lower degree of orientation, suggest that the donor regions may be largely amorphous when heating is at 800 °C. The reaction is probably not one of stoichiometric disproportionation, but a conversion of parts of the crystal into β-$CaSiO_3$ at the expense of donor regions which remain largely amorphous. The mean Ca:Si ratio of these donor regions could then have any value above 4:3. On this ratio would depend the proportion of foshagite which is converted into β-$CaSiO_3$; consequently this proportion is not stoichiometrically defined. There is a tendency, but probably no more than this, for β-Ca_2SiO_4 to crystallize from the amorphous material in the donor regions. At least two explanations are possible for the preferred orientation of the β-Ca_2SiO_4. It may occur because the bulk of the donor material is not completely amorphous, but retains some degree of structure. Alternatively, the orientation of the β-Ca_2SiO_4 crystals may be determined by that of the newly formed β-$CaSiO_3$. In the latter case, the crystallization of the β-Ca_2SiO_4 would occur by a sort of internal epitaxial process. Similar mechanisms to the above can readily be postulated to explain the transformation of xonotlite into β-$CaSiO_3$, and other transformations that occur in the same temperature region. Mamedov & Belov (1958) considered a single chain structure for foshagite to be unlikely on the grounds that it did not permit a simple explanation of the dehydration process. As has been shown here, it explains this process very simply if the hypothesis of stable $Ca(O, OH)_2$ layers and migration of intervening Si and oxygen is accepted. It probably does not permit of a simple explanation if the Si–O bonds and not the Ca–O bonds are assumed to be the most stable elements during the transformation. Mamedov & Belov appear to have based their arguments on the latter assumption, but there is reason to believe that it is incorrect.

We thank Dr F. Liebau (Institut für anorganische Chemie, Berlin-Adlershof) for valuable advice on the structure determination.

References

Buerger, M. J. (1956). *Proc. Nat. Acad. Sci. Wash.* **42**, 113.

Dent, L. S. & Taylor, H. F. W. (1956). *Acta Cryst.* **9**, 1002.

Dornberger-Schiff, K. (1956). *Acta Cryst.* **9**, 593.

Dornberger-Schiff, K., Liebau, F. & Thilo, E. (1955). *Acta Cryst.* **8**, 752.

Eakle, A. S. (1925). *Amer. Min.* **10**, 97.

Gard, J. A. & Taylor, H. F. W. (1958). *Amer. Min.* **43**, 1.

Gard, J. A., Taylor, H. F. W. & Staples, L. W. (1960). Proc. 4th Int. Cong. of Electron Microscopy (Berlin 1958), **1**, 449.

Gard, J. A. & Taylor, H. F. W. (1959). *Nature, Lond.* **183**, 171.

Jeffery, J. W. (1953). *Acta Cryst.* **6**, 821.

Mamedov, Kh. S. & Belov, N. V. (1955). *Doklady Akad. Nauk S.S.S.R.* **104**, 615.

Mamedov, Kh. S. & Belov, N. V. (1956*a*). *Zap. Vses. Miner. Obšč.* **85**, 13.

Mamedov, Kh. S. & Belov, N. V. (1956*b*). *Doklady Akad. Nauk S.S.S.R.* **107**, 463.

Mamedov, Kh. S. & Belov, N. V. (1958). *Doklady Akad. Nauk S.S.S.R.* **121**, 901.

Tarte, P. (1959). Private communications, 3 September and 9 October.

Taylor, H. F. W. (1958). *Z. angew. Chem.* **70**, 320.

Tolliday, J. (1958). *Nature, Lond.* **182**, 1012.